Available online at www.sciencedirect.com

ScienceDirect

Procedia Manufacturing 26 (2018) 1459–1470

Procedia MANUFACTURING

www.elsevier.com/locate/procedia

46th SME North American Manufacturing Research Conference, NAMRC 46, Texas, USA

Tool wear prediction in end milling of Ti-6Al-4V through Kalman filter based fusion of texture features and cutting forces

Kunal Tiwari, Ameer Shaik and Arunachalam N*

Department of Mechanical Engineering, IIT Madras, Chennai, Tamil Nadu, 600036, India

* Corresponding author. Tel.: +91-44-2257-4722 .
E-mail address: chalam@iitm.ac.in

Abstract

The current trend of Industry 4.0 development requires an integration of the process sensing technologies with the cloud computing network to design the cyber-physical systems which can seamlessly transfer data between the connected devices. This will pave a way for real-time process monitoring as well as the control of the process by the use of decision-making algorithms. The current paper explores the opportunities with this regard in the area of tool wear prediction in end milling of Ti-6Al-4V alloy at various operating conditions. A series of slot milling passes were made at various parameter combinations of feed, speed, and depth of cut until the flank wear on tool crosses the failure criterion. The cutting force data acquired in the process with the dynamometer and the texture features from the image of the milled surface are used to build a model for predicting the flank wear through the Kalman filter approach. The fusion model built using the Kalman filter methodology achieves a good accuracy in predicting the flank wear on the tool. The model is highly accurate in predicting the wear as the tool approaches the failure threshold. Thus the model can enable the decision control module to trigger a tool change signal and improve the overall productivity of the process.

Peer-review under responsibility of the scientific committee of the 46th SME North American Manufacturing Research Conference.

Keywords: Industry 4.0; End milling; Texture analysis; Kalman filter; Wear prediction

1. Introduction

The product quality of parts is of utmost importance during any machining process. The surface finish of the machined parts is directly influenced by tool wear. Tool wear detection and prediction during machining are of prime importance in ensuring the quality of parts being machined by preventing their machining by a worn-out tool. This also helps in avoiding material wastage by reducing improper machining of components. Reliable estimation of tool wear during machining will

2351-9789
Peer-review under responsibility of the scientific committee of the 46th SME North American Manufacturing Research Conference.
10.1016/j.promfg.2018.07.095

significantly enhance the productivity of the process by providing a trigger for the change of a worn-out tool. Various condition monitoring approaches involving the use of multiple sensors have been used to monitor the process variables during machining for estimating tool wear. Nouri *et al.* [1] have presented a cutting condition independent method for estimating tool wear in real-time by correlating the force model coefficients with the wear state. A time series model was developed by Altintas [2] for detecting tool breakages by monitoring of cutting forces in milling. Yao *et al.* [3] have also developed a trivariate Autoregressive Moving Average Vector (ARMAV) time series models by analyzing dynamic cutting force in oblique machining for a comprehensive estimation of tool wear.

A tool wear observer model was developed by Chen and Li [4] by correlating cutting force components with the flank wear width during the milling of nickel-based alloys. Kuljanic and Sortino [5] have also proposed a method for estimating tool wear in face milling by analyzing the feature parameters of the cutting force signals.

Ghosh *et al.* [6] have developed a sensor fusion model comprising of various machining signals like cutting forces, spindle vibration, spindle current and sound pressure level to estimate the flank wear in milling. Cuka and Kim [7] have also proposed a Fuzzy Inference system (FIS) comprising of the same machining signals like cutting forces, spindle current, spindle vibration and machining sound from microphone to estimate tool wear in end milling.

A general drawback of many condition monitoring techniques is that some sensors are not suitable for use in the live production environment. Thus there is a scope for development of non-contact type monitoring systems which can monitor the surface of the part after machining. Machine vision systems are well suited for the purpose as they can capture images of the surface being machined in real time thereby aiding in the automation of the process.

A machine vision system generally consists of a camera accompanied with an illumination system and a frame grabber for acquiring an image [8]. The surface images captured through the machine vision systems can be analyzed through texture analysis methods to relate to the variation in tool wear. This method can provide valuable insights into the cutting process because the cutting tool leaves behind an imprint during machining which contains information about the machining condition along with the current condition of tool wear. This relationship can be further analyzed to estimate the tool wear during the machining process. The tool wear detection method can also be used to trigger the Automatic Tool Changer (ATC) to establish automation in the process itself. This decision-making module along with a real-time image processing setup can be used in the production line. The components being machined can be thus scanned continuously by a camera with an illumination setup. This indirect measurement of wear is advantageous as the tool wear state is determined without interrupting the process. The surface texture of the acquired image is processed in real-time and based on the threshold criterion the decision setup can trigger the ATC to command a tool change. The image data is also continuously streamed to a cloud-based data storage and learning architecture. This enables the remote monitoring and control of the production process by mobile devices. The devices can thus view the current state of tool wear along with remaining useful life (RUL) estimation based on the predictive models.

Thus the analysis of texture features from the image of the surface being machined can bring about productivity improvements in the production environment. Researchers across the world have proposed a variety of techniques for analyzing texture features. These analysis techniques are mainly divided into three categories: statistical, structural and spectral methods.

The statistical approaches are based on characterizing the texture through various statistical features while defining them as a stochastic process. Generally, image features have been extracted from the grey level histogram of the image. Haralick *et al.* [9] have proposed grey-level co-occurrence matrix (GLCM) as a statistical method to determine the texture features. Gadelmawla *et al.* [10] have used the GLCM technique to calculate the time for which cutting tools have been used in turning. This was done by identifying the texture parameters which have a high correlation with the machining time.

The structural methods for texture analysis are based on distinguishable features like a group of parallel lines in an image having a periodic pattern. The texture definition is thus given by location and characteristic patterns in the image [11]. One class of the structural methods is the column projection analysis. This is suitable for cases where the texture feature is given by regularly spaced lines during machining by a fresh tool. However, with tool wear,

this periodicity is lost leading to an irregular texture. The other structural method is the fast Hough transform. The images of machined surfaces having line segments of different varieties can be detected by Hough transform to a good effect [12]. Kassim *et al.* [13] have predicted the tool condition from the texture features extracted from surface images of machined parts by combining the artificial neural network (ANN) with Hough transform.

The spectral texture analysis techniques are based on analyzing the frequency content of the intensity of the available pixels in an image. Dong-Chen He *et al.* [14] have used the texture spectrum from the image to identify the texture features. A two dimensional Fourier transform was used by Du-Ming Tsai *et al.* [15] to extract the textural features in the frequency domain for relating to the surface roughness.

The present study comprises the end milling of Ti-6Al-4V alloy with carbide inserts having TiAlN coating. Titanium alloy (Ti-6Al-4V) is the most widely used alloy in the aerospace, automobile and biomedical industries due to its inherent properties like high strength to weight ratio and corrosion resistance. However, machinability of Ti-6Al-4V remains challenging owing to its low thermal conductivity which leads to high cutting temperatures. Titanium can also weld with the cutting tool during machining because it is chemically reactive. Thus tool wear is significant during machining of titanium which necessitates for a need to develop an accurate detection system for tool wear to maximize the productivity during machining.

The overall vision is depicted in Fig. 1 where the CNC high-speed milling machine is monitored for cutting forces and flank wear during machining. The statistical methods are employed for surface image analysis. The operating conditions and machining time along with the features selected from force and image analysis form the basis for building a prognostic model to estimate the remaining useful life (RUL) of the tool based on the current state of wear. The decision module can alarm the need for a change of tool if wear (V_B) crosses the threshold (V_C). If the wear (V_B) is below the threshold value, it can direct the milling process to continue with the same tool until the flank wear on tool crosses the threshold criterion. The current work is focused on this aspect only by developing a relationship between the image texture features and cutting force data with tool wear. Also, this relationship is combined with the wear estimations from the volume of material removed in each pass to establish an improved wear prediction model using the Kalman filter approach.

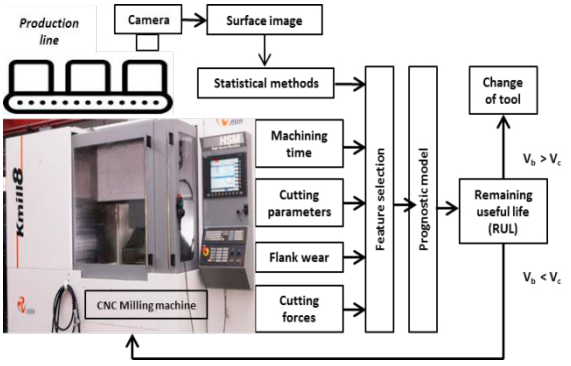

Fig. 1.Prognostic model development for high-speed milling machine

2. Experimental details

The milling experiments were conducted on Jyoti KMill8 high-speed milling machine using TiAlN coated carbide end mill inserts (Kennametal LNGU110408ERGE, KC725M) with a 16 mm diameter 2-insert type end mill cutter (Kennametal M4D016Z02A16LN11L090). The work material used was Ti-6Al-4V alloy. The parameter combinations for the conducted experiments are listed in Table 1.

Table 1. Milling conditions for all experiments

Experiment No.	Cutting speed v (m/min)	Table feed f (mm/min)	Depth of cut a_p (mm)
1	300	150	0.75
2	325	150	1.00
3	350	150	1.25
4	300	200	1.00
5	325	200	1.25
6	350	200	0.75
7	300	250	1.25
8	325	250	0.75
9	350	250	1.00

The experiments involved milling slots of 16 mm diameter in multiple passes. The force values for each machining pass were recorded using a three-component Kistler 9257B dynamometer at a

sampling rate of 16 kHz. After every pass, the tool wear measurement for both the inserts was done using Zeiss Stemi-2000CS stereo microscope at a 40x magnification. Each experiment was performed with a fresh pair of inserts and multiple passes were done until the average flank wear (VB_{avg}) failure criterion of 0.3 mm was reached for the tool. The failure criterion of 0.3 mm is based on ISO 8688-2:1989 standard for tool life testing in end milling [16]. It recommends the tool life endpoint as 0.3 mm averaged over all teeth for uniform wear. This failure criterion has been used by Garcia and Ribeiro [17] during the end milling of Ti6Al4V. Polini and Turchetta [18] have also defined the end of tool life when the average flank wear reached 0.30 mm or when a catastrophic fracture of the edge was observed. The experimental setup is shown in Fig. 2.

All the high-speed experiments were conducted with coolant flow to minimize high temperatures involved during machining of titanium. Also for each slot, images of the milled surface at a resolution of 1388 x 1038 were taken using the same stereo microscope with a 32x magnification for texture analysis. Each image was then cropped to 256 x 256 pixels before processing in MATLAB® environment. These steps in achieving the required cropped image are shown in Fig. 3.

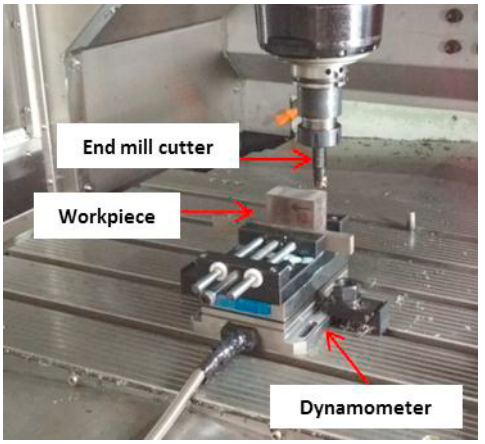

Fig. 2. Experimental setup for milling along with dynamometer

3. Methodology

Various texture analysis methods are useful in extracting the details in an image to identify the features of interest. The texture represented by the intensity distribution of pixels in the captured image is utilized to determine the texture features. These features can be used to gain insight into the process by texture analysis. The present work involves the selection of such features of interest for predicting the tool wear based on the Grey level co-occurrence matrix (GLCM) and a histogram of an image.

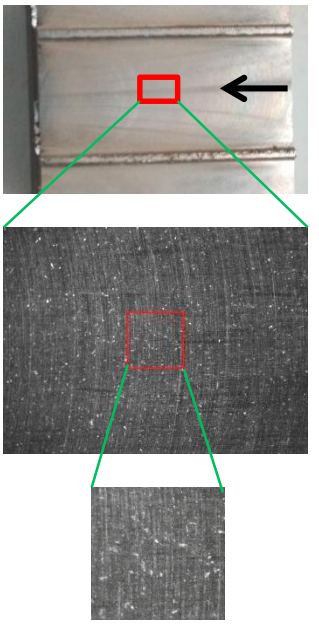

(a) Surface of the milled workpiece (Arrow indicates the machining direction over length of 35 mm)

(b) Image of the milled surface from stereo microscope (Size: 1388 x 1038 pixels)

(c) Cropped image in MATLAB® (Size: 256 x 256 pixels)

Fig. 3. Steps involved in achieving cropped image for analysis during experiment: 1 (t = 183.6 s)

3.1. Histogram parameters

The image histogram is a plot of the grey levels and their frequency of occurrences in the image. Variance and energy are selected as the first order statistical parameters based on their monotonic trend with time. These are defined as [19]:

$$Variance\ (\sigma^2) = \frac{1}{N_x N_y} \sum_{N_g=0}^{255} (N_g - \mu)^2 H(N_g) \quad (1)$$

$$Energy = \frac{1}{N_x N_y} \sum_{N_g=0}^{255} H(N_g)^2 \quad (2)$$

Here μ and σ are the mean and standard deviation of the histogram respectively, while the size of the image is represented by N_x and N_y. Also, the number of grey levels is represented as N_g and their frequency of its occurrences are given by $H(N_g)$.

3.2. Grey level co-occurrence matrix (GLCM) approach

GLCM is a second-order statistical approach which was proposed by Haralick *et al.* [9]. It is a two-dimensional (2D) matrix which characterizes the influence of the grey level pattern surrounding the given pixel. The size of GLCM matrix denotes the number of grey levels present in the image. A pair of grey level values occurring at a specified distance and direction is identified by this approach [19]. GLCM calculation involves the consideration of two or more neighboring pixels to identify the relationships in grey level. The present study is based on analyzing this relationship along $\theta = 0°$ direction where θ is the orientation parameter for two adjacent pixels. This is done to ensure that the lay marks in the surface image are oriented vertically with respect to the orientation parameter of $\theta = 0°$. The offset distance is kept at $d = 1$ pixel for analyzing pixels lying on side of each other. Entropy and diagonal moment of GLCM are selected as features of interest based on a monotonic trend with time. They are defined by following equations [19]:

$$Entropy = -\sum_{i=1}^{N_g}\sum_{j=1}^{N_g} P(i,j)\log\big(P(i,j)\big) \quad (3)$$

$$Diagonal\ moment(DM) = \sum_{i=1}^{N_g}\sum_{j=1}^{N_g}\sqrt{\frac{1}{2}|i-j|P(i,j)} \quad (4)$$

Here the normalized GLCM of the image is represented by *P(i, j)* and *(i, j)* represent the indices combinations of grey level values. A normalization factor R is calculated for normalizing the GLCM. The present study is based on the nearest horizontal neighbor ($d = 1$, $\theta = 0°$) for calculating the normalization factor *R*.

3.3. Grey level average (Ga)

Many researchers have used the grey level average (*Ga*) as a statistical parameter for surface roughness prediction of machined surfaces. Grey level average as proposed by Younis [20] is expressed as:

$$Ga = \frac{1}{N_x N_y}\sum_{i=1}^{N_x}\sum_{j=1}^{N_y}|M(i,j)| \quad (5)$$

Here the size of the image is given by N_x and N_y and the deviation of grey level from the mean value of the surface image is denoted by *M(i, j)*.

3.4. Kalman filter

The Kalman filter is an estimator which is stochastic in nature. It integrates the feedback from predicted values to improve the estimates [21, 22]. Möhring *et al.* [23] have calculated states of the system which are inherent by using a measurement system which has known inputs and outputs along with noise content. The use of this technique leads to noise reduction also as expected by a filter. The state space description of the system is described by the following equation:

$$x_k = Ax_{k-1} + Bu_{k-1} + w_{k-1} \quad (6)$$

Here *B* is a matrix relating the inputs *u* available at a previous time step to the current state, *A* represents a matrix relating the states available at the previous time step of *k-1* to the current time step (*k*), , and *w* is the noise in estimation of states. The noise is assumed to follow a normal distribution. This is described in the following equation having zero mean and a covariance matrix *Q*:

$$w_k \sim N(0, Q) \quad (7)$$

The modeled discrete measurement equation is stochastic in nature. The current state is thus compared to the measured signals as depicted by the following equation:

$$z_k = Hx_k + v_k \quad (8)$$

$$v_k \sim N(0, R) \quad (9)$$

Here *H* is a matrix relating the recent measurements to the current states and v_k is the measurement noise. This noise follows a normal distribution with zero mean and covariance *R*, while the measured signal is denoted as z_k

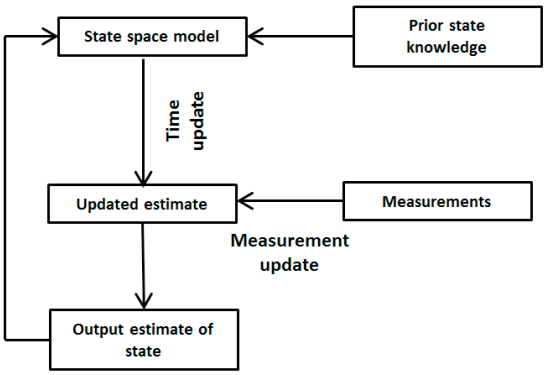

Fig. 4. Kalman filter methodology

Kalman filter initially starts with some deduced prior state information available at time *k*. Its state gets updated based on the knowledge at a previous time step of *k-1*. The prior state is updated to find the posterior state as more measurements are available. The time update is the first update to the system. The next update is the measurement update to calculate the posterior state. This process does not need a new set of measurements as it is a recursive process as depicted in Fig. 4. Niaki *et al.* [24] have used the spindle power information with this Kalman filter methodology to predict tool flank wear in cutting hard-to-machine gamma-prime strengthened alloys.

4. Results and Discussions

The average flank wear values for all experiments were plotted and shown in Fig. 5. It is evident from all the wear propagation plots that the average flank wear increases with machining time which is as expected. However, the rate of wear propagation differs due to the changes in the operating conditions.

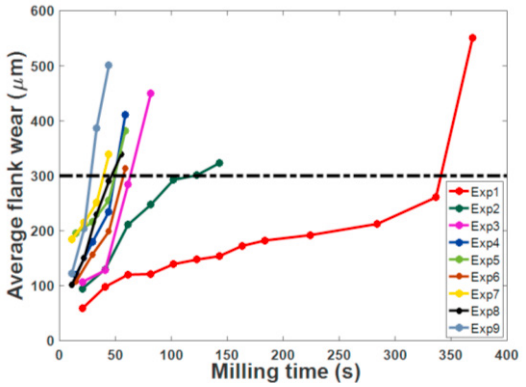

Fig. 5. Tool wear propagation plots for all experiments

4.1. Analysis of cutting force data

The average force values in three directions (F_x, F_y, and F_x) were used to achieve the resultant force for each pass of slot milling. The force values along with the corresponding tool wear for the experiment: 1 are listed in Table 2. The resultant force F_r was calculated by the following equation:

$$F_r = \sqrt{F_x^2 + F_y^2 + F_z^2} \quad (10)$$

The variation of the resultant of cutting force with milling time is also shown in Fig. 6. Also, the wear images for insert-1 at different time stages of milling are shown in Fig. 7. The average flank wear was measured on the two inserts after each pass. As the same two inserts were used in the end mill cutter in each consecutive pass, the average flank wear for that pass was calculated as the average of measured wear on both the inserts.

Table 2. Average wear and force values for experiment: 1

Milling time, t (s)	Avg flank wear (μm)	Avg F_x (N)	Avg F_y (N)	Avg F_z (N)	Resultant force F_r (N)
20.4	58.65	68.18	60.46	86.21	125.45
40.8	98.15	92.52	81.98	130.42	179.70
61.2	120.21	84.30	64.14	123.55	162.75
81.6	121.37	68.73	55.76	111.28	142.18
102	139.38	74.92	54.56	110.54	144.25
122.4	147.51	67.56	49.23	95.15	126.65
142.8	153.89	67.08	50.94	96.01	127.73
163.2	172.47	59.39	49.83	87.04	116.56
183.6	182.35	56.62	49.00	83.63	112.25
224.4	192.22	62.75	49.85	82.29	114.86
284	212.55	83.97	65.45	98.41	144.97
336.4	260.75	182.71	149.03	200.58	309.55
369.2	551.11	281.82	252.52	380.20	536.41

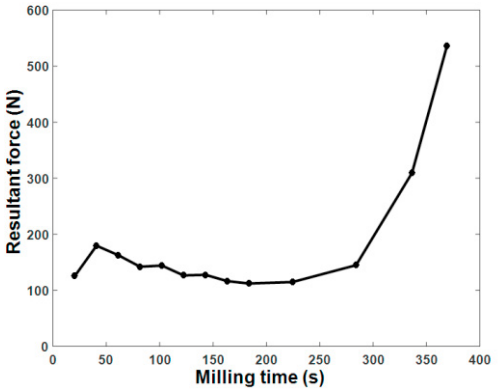

Fig. 6. Variation of resultant force with milling time

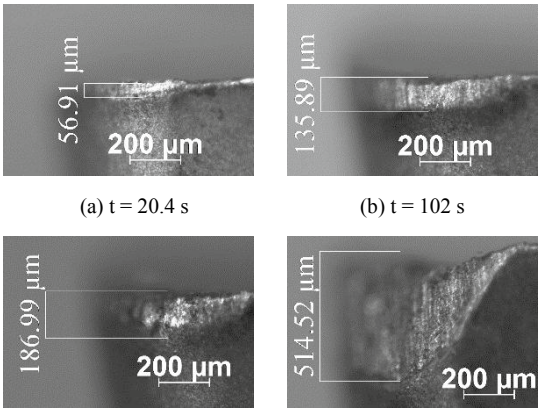

(a) t = 20.4 s (b) t = 102 s

(c) t = 183.6 s (d) t = 369.2 s

Fig. 7. Flank wear measurement (microns) for insert-1 at various time stages of milling

4.2. Texture feature analysis

The images of the milled surface show a change in the pattern as the tool wear increases. Initially, as the tool is fresh, the milled surface has uniform lay marks but as the milling progresses the pattern periodicity is lost in greyscale images. The images of the milled surface with constant illumination captured at various intervals corresponding to the tool wear measurement for the experiment: 1 are shown in Fig. 8.

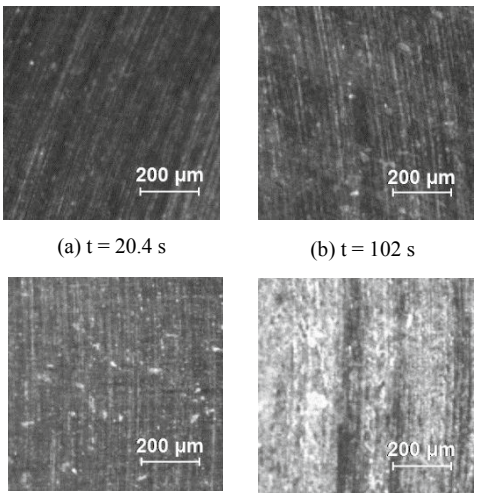

(a) t = 20.4 s (b) t = 102 s

(c) t = 183.6 s (d) t = 369.2 s

Fig. 8. Surface images at various stages of milling

Various texture features as described earlier were calculated for the images from each experimental pass through the image histogram, grey level average, and GLCM approaches. The statistical features like variance, energy, entropy (GLCM), diagonal moment (GLCM) and grey level average (Ga) were selected for milled surface image analysis. These features were selected because they had monotonic increasing or decreasing trend with machining time and thereby useful in model building. The plots of selected features are shown in Fig 9-13. These variations can be attributed to the changes in intensity values of grey levels along with their frequency of occurrences in the image of the milled surface as the tool keeps wearing. Initially, the milled surface has a regular feature pattern due to which the pixel intensities are concentrated in a narrow range. But as the milling progresses, the pixel intensities are dispersed over a wider range.

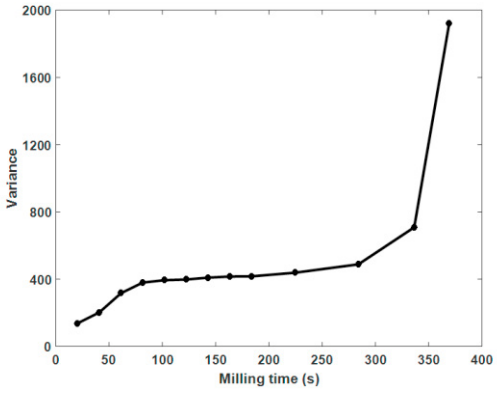

Fig. 9. Variation of histogram variance with milling time

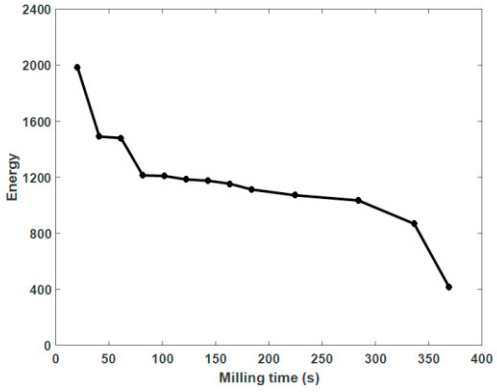

Fig. 10. Variation of histogram energy with milling time

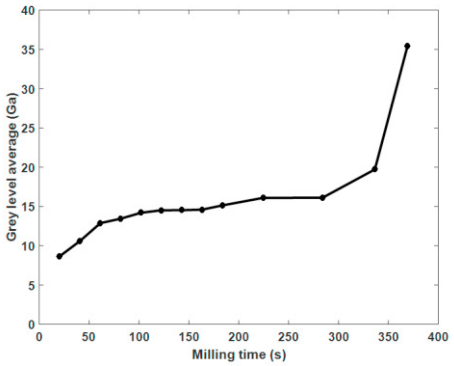

Fig. 11. Variation of Grey level average with milling time

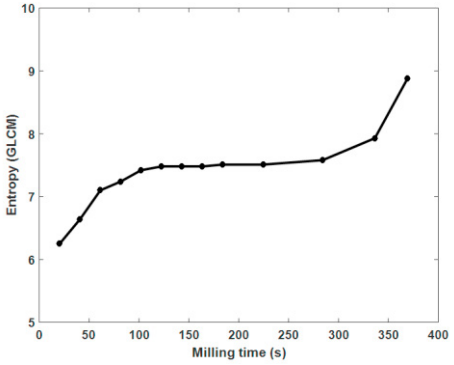

Fig. 12. Variation of entropy (GLCM) with milling time

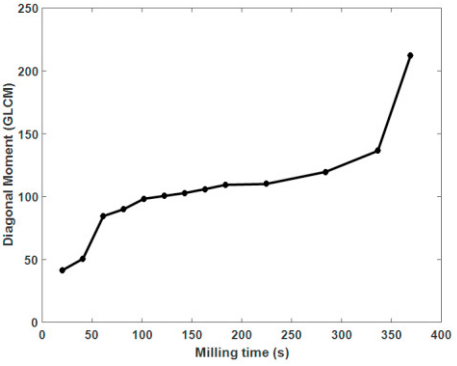

Fig. 13. Variation of diagonal moment (GLCM) with milling time

The histogram variance has an increasing trend with time because the tool wear causes the image pattern to lack periodicity. As the grey level intensities keep on getting distributed, the variance keeps increasing. Also, the histogram energy decreases with time because initially, the image has fewer grey level values which get dispersed as milling progresses. The grey level average (Ga) parameter increases with time because the number of pixels with greater deviation from mean value increases too with time as the dispersion of grey level values keeps increasing. Initially, the GLCM matrix has few combinations of grey level pairs with high occurrence frequencies owing to the regular surface texture. But as the milling progresses, the entropy and diagonal moment parameters of GLCM show an increasing trend with time as the spread of occurrence frequencies of grey level pairs keeps increasing, depicting the loss of texture periodicity.

4.3. Predictive model using Kalman filter

This section describes the development of Kalman filter based model for tool wear prediction. The cutting force, histogram variance and cumulative volume of material removed data from the experiment: 1 (v=300 m/min, f =150 mm/min, a_p =0.75 mm) are used to develop a model for flank wear. The variance data is selected among the various image features owing to its monotonicity and high correlation of 0.985 with flank wear. Apart from having a high correlation with wear, it is also significant in predicting wear based on regression tests. Linear regression models built between the wear and variance models for all experiments suggested the significance of wear prediction from variance as the *Significance F value* was found to be less than 0.1 ranging from 8.19 E-10 to 0.078. Also, the R squared values were above 0.8 for all cases suggesting a good fit in predicting wear. Thus histogram variance is a suitable parameter for estimating wear. The volume of material removed (V_m) for each pass during slot milling is calculated by the following equation:

$$V_m = d_c a_p l \qquad (11)$$

Here d_c is the diameter of the cutter (mm), a_p is the axial depth of cut (mm) and l is the length of the machining pass (mm). Table 4 lists the average flank wear, resultant force, histogram variance and cumulative volume of metal removed for each pass of slot milling of the experiment: 1 used for model building. The first step involved building a linear regression model with cumulative volume of material removed (V_{cm}) as the predictor variable and average flank wear as the response variable. This model is used to estimate the initial wear ($\hat{x}_0$) in the Kalman model. This regression model is as follows:

$$VB_{avg} = 43.553 + 0.0396V_{cm} \qquad (12)$$

Next, another linear regression model relating average flank wear with resultant force (F_r), histogram variance (G) and milling time (t) was developed and the predictions from this are used as the measurement signal. The regression equation for this model is as follows:

$$VB_{avg} = 34.534 - 0.0559F_r + 0.2353G + 0.2503t \quad (13)$$

Tool wear predictions using the regression model from Eq. (13) were improved by incorporating a Kalman filter model. The prediction from the linear regression model given by Eq. (12) was used as the initial estimate for the Kalman model. For one-dimensional state, the Kalman filter equations [24] are defined as:

$$\hat{x}_k^- = A\hat{x}_{k-1} \quad (14)$$

$$P_k^- = AP_{k-1}A^T + Q \quad (15)$$

These two equations constitute the prediction stage of the Kalman filter. After prediction, the correction equations [24] follow which are given by:

$$K_k = \frac{P_k^- H^T}{HP_k^- H^T + R} \quad (16)$$

$$\hat{x}_k = \hat{x}_k^- + K_k(z_k - \hat{x}_k^-) \quad (17)$$

$$P_k = (I - K_k H)\, P_k^- \quad (18)$$

Table 4. Average flank wear, resultant force, histogram variance and cumulative volume of material removed for experiment: 1 (v =300 m/min, f =150 mm/min, a_p =0.75 mm)

Milling time, t (s)	Average flank wear (μm)	Resultant force F_r (N)	Histogram variance	Cumulative volume of material removed (mm^3)
20.4	58.65	125.45	137.43	420
40.8	98.15	179.70	202.35	840
61.2	120.21	162.75	316.86	1260
81.6	121.37	142.18	379.81	1680
102	139.38	144.25	393.79	2100
122.4	147.51	126.65	397.82	2520
142.8	153.89	127.73	408.96	2940
163.2	172.47	116.56	415.61	3360
183.6	182.35	112.25	416.79	3780
224.4	192.22	114.86	438.35	4812
284	212.55	144.97	488.22	6408
336.4	260.75	309.55	708.31	7788
369.2	551.11	536.41	1920.33	8580

Thus each step of the Kalman filter comprises of a prediction stage and a correction stage for reducing the error in further predictions. The current estimated wear state ($\hat{x}_k^-$) is defined as a function of previous optimum wear state ($\hat{x}_{k-1}$) using the state transition matrix (A).

The initial optimum estimate of signal ($\hat{x}_0$) is found from Eq. (12) which is the wear-volume model. Since there is no control input, the control signal (u_k) is also zero. The initial guess estimate for wear is taken as 90 μm based on the observations from the experimental data. The state transition matrix (A) is based on the average rate of increase of wear in the experimental data. The initial estimation error variance P_0 for the model is taken as the square of error between the initial guess estimate of wear and estimated wear value from the Eq. (12). The variance (Q) of process noise is found as the variance of wear estimates from the Eq. (12). The transformation matrix (H) is taken as 1 because the measured signal here is the wear value itself from Eq. (13). The variance (R) of the measurement noise is calculated as the variance of wear estimates from Eq. (13). The values of the model parameters are given in Table 5.

Table 5. Parameters in the Kalman model

Parameter	Value
A	1.236
P_0	887.0801
Q	1.0824e+04
H	1.00
R	1.2978e+04

The output from the linear regression model given in Eq. (13) is the measured signal (z_k) while K_k is the Kalman gain in each step. The optimal estimates of wear were obtained using this Kalman gain in each step. The force data used in the measured signal given by Eq. (13) is found to be not significant because of the high p-value (0.412) of its coefficient. Thus another regression model relating average flank wear with histogram variance and time was developed excluding the force data. The model equation is given below:

$$VB_{avg} = 31.087 + 0.2202G + 0.257t \quad (19)$$

This model was used in place of the model from Eq. (13) as the measured signal (z_k) for wear with the same Kalman methodology to present another case of model predictions. The results of tool wear

predictions for these two cases of measured signal are plotted in Fig. 14. The wear predictions from the measured signal including the resultant force given by Eq. (13) is referred to as Kalman model with force in the graph. The wear predictions from the measured signal excluding the resultant force given by Eq. (19) is referred to as Kalman model without force. The tool failure criterion for average flank wear of 300 µm was used as a threshold value to signal the change of worn-out tool.

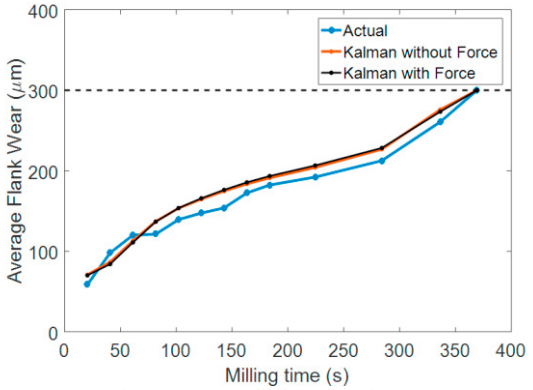

Fig.14 Wear prediction (experiment: 1)

The robustness of the model was verified by repeating the cutting condition of experiment: 1 (v =300 m/min, f =150 mm/min, a_p =0.75 mm) as repetition experiment: 1. The histogram variance, resultant force and cumulative volume of material removed data along with the milling time for this repetition experiment was used with the Kalman filter methodology described above to predict the flank wear. The results comparing the performance of the two discussed Kalman models, one with force and other without force are plotted in Fig. 15.

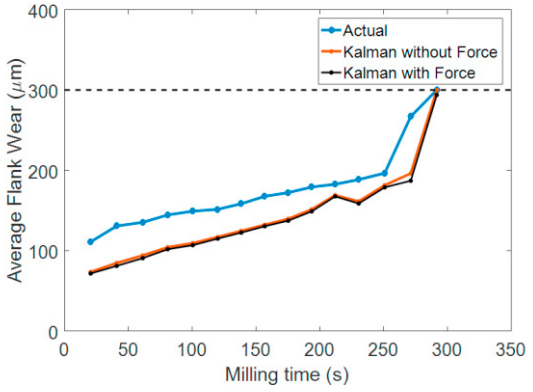

Fig.15 Wear prediction (repetition experiment: 1)

Similarly both Kalman models were also used with the force, variance, milling time and volume of material removed data obtained during experiment: 2 (v =325 m/min, f =150 mm/min, a_p =1 mm) and experiment: 3 (v =350 m/min, f =150 mm/min, a_p =1.25 mm). The wear prediction results corresponding to these two experiments are given in Fig. 16-17.

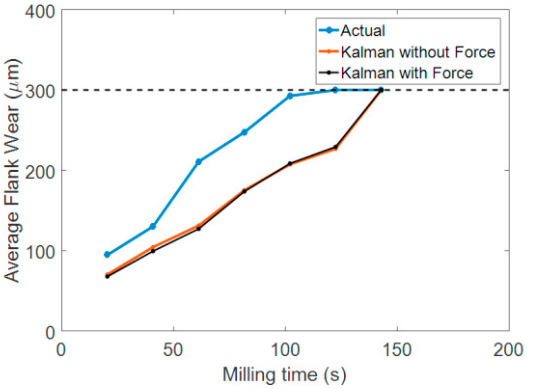

Fig.16 Wear prediction (experiment: 2)

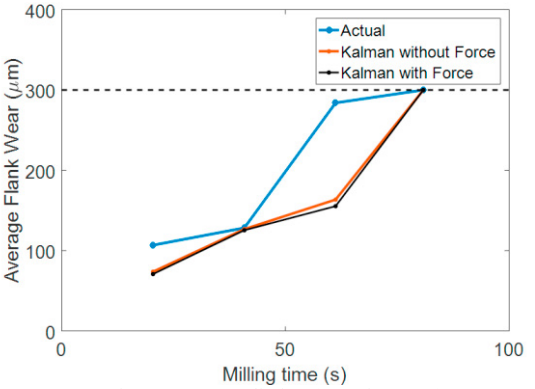

Fig.17 Wear prediction (experiment: 3)

Table 6. Comparison of RMSE in predictions of wear (µm)

Experiment No.	Kalman with force	Kalman without force
1	14.1729	13.2956
Repetition 1	39.7165	36.5552
2	61.1828	60.2675
3	66.7718	62.4369

It is evident from all of the above wear prediction plots that Kalman filter predicts tool failure state accurately. Thus it can be used to trigger the ATC for tool change as the tool gets worn-out. It is also observed that both Kalman models, with and without force follow the same trend in predicting wear in all the cases. The performance of both the models for the

discussed experiments is compared on the basis of RMSE in predicting wear as given in Table 6. It is observed that the RMSE reduces when excluding the force data from the measured signal equation. This is because, the regression coefficient for the resultant force in Eq. (13) is not significant based on its high p-value. Thereby considering a higher setup cost associated with a standard dynamometer, it is not advantageous to use the force data for modeling. The developed Kalman model without force generalizes well for different experimental conditions in predicting tool failure state at a constant feed rate, f =150 mm/min from the Fig. 14-17. However, the model has a limitation that it cannot predict accurately at higher combinations of feed rates because sufficient data points for model training are not available at higher feed rate conditions.

The present work does not include experimentation at lower cutting speeds. Further research in this area would be directed at modeling the wear at lower cutting speeds. The effect of various operating conditions is captured in the information from the texture feature obtained from the surface image. This enables good predictions of tool wear state in conjunction with a cumulative volume of material removed in the developed Kalman model.

The present model cannot be generalized be as such to different cutting tool and coating materials as well as to different workpiece materials. Further experiments should be conducted for a chosen combination of tool and workpiece materials at different cutting conditions and then a similar methodology can be adopted to model wear. This methodology can also be extended to tools with different geometries because the effect of process parameters like cutting speed, feed and depth of cut is captured in the cutting force data and the texture features. Thus the texture features from these images can serve as fingerprints to predict wear as they correspond to the current wear state.

5. Conclusion

In the present study, the cutting force and image texture data from the milled surface are utilized to build a model for predicting average flank wear. Initially, the significant texture features like histogram variance, energy, grey level average (Ga), entropy (GLCM) and diagonal moment (GLCM) showing correlation with wear are selected for relating the effect of tool wear to the milled surface image. Among these, the histogram variance was selected as the texture parameter for building the prediction model based on its high correlation and significance in linear regression with wear. The surface image can serve as a fingerprint to identify the tool wear state. This idea is demonstrated by combining the histogram variance with resultant cutting force data through Kalman filter approach to develop a predictive model for flank wear estimation.

The initial estimates of wear were obtained using a linear regression model for flank wear with a cumulative volume of material removed in each pass. Two cases of Kalman filter modeling are presented, one with force and other without including the force data. It was observed that both models were able to predict the tool failure progression. The robustness of the developed model was evaluated by performing a repetition experiment with the same cutting conditions as the training dataset. The data from the other two experiments at the same feed rate of 150 mm/min was used with the model to predict wear.

It was observed that the Kalman model with just histogram variance and milling time has good accuracy in predicting flank wear in all the cases. This suggests the exclusion of force data from the modeling taking into account the setup cost associated with the dynamometer. It was also observed that the use of resultant force data alone was not suitable for the prediction of wear in the present study.

The predictions from the Kalman filter model keep improving as the tool nears its failure criterion of 0.3 mm of average flank wear, thereby suggesting the adoption of the approach for predicting the time to failure of the tool in cases where sufficient data points are available like in lower cutting speeds and feed rates. This would enable timely replacement of the tool to improve the productivity of the process by efficient scheduling. As the machining process is stochastic, the texture feature selected for building the wear model have to be chosen based on their significant relationship with wear propagation. Thus, the methodology can also be further extended by combining other features to increase the reliability of overall wear estimates.

References

[1] M. Nouri, B. K. Fussell, B. L. Ziniti, E. Linder, Real-time tool wear monitoring in milling using a cutting condition independent method. International Journal of Machine Tools and Manufacture, 89, (2015) 1-13.

[2] Y. Altintas, In-process detection of tool breakages using time series monitoring of cutting forces. International Journal of Machine Tools and Manufacture, 28(2), (1988) 157-172.

[3] Y. Yao, X. D. Fang, & G. Arndt, Comprehensive tool wear estimation in finish-machining via multivariate time-series analysis of 3-D cutting forces. CIRP Annals-Manufacturing Technology, 39(1), (1990) 57-60.

[4] X. Q. Chen, H. Z. Li, Development of a tool wear observer model for online tool condition monitoring and control in machining nickel-based alloys. The International Journal of Advanced Manufacturing Technology, 45(7-8), (2009) 786-800.

[5] E. Kuljanic, M. Sortino, TWEM, a method based on cutting forces—monitoring tool wear in face milling. International Journal of Machine Tools and Manufacture, 45(1), (2005) 29-34.

[6] N. Ghosh, Y. B. Ravi, A. Patra, S. Mukhopadhyay, S. Paul, A. R. Mohanty, A. B. Chattopadhyay, Estimation of tool wear during CNC milling using neural network-based sensor fusion. Mechanical Systems and Signal Processing, 21(1), (2007) 466-479.

[7] B. Cuka, D. W. Kim, Fuzzy logic based tool condition monitoring for end-milling. Robotics and Computer-Integrated Manufacturing, 47(C), (2017) 22-36.

[8] S. Dutta, S. K. Pal, R. Sen, On-machine tool prediction of flank wear from machined surface images using texture analyses and support vector regression. Precision Engineering, 43 (2016) 34-42.

[9] R. M. Haralick, K. Shanmugam, Textural features for image classification. IEEE Transactions on systems, man, and cybernetics, 6 (1973) 610-621.

[10] E. S. Gadelmawla, F. A. Al-Mufadi, A. S. Al-Aboodi, Calculation of the machining time of cutting tools from captured images of machined parts using image texture features. Proceedings of the Institution of Mechanical Engineers, Part B: Journal of Engineering Manufacture, 228.2 (2014) 203-214.

[11] K. T. Kumar, N. Arunachalam, L. Vijayaraghavan, Prognostics model for tool life prediction in milling using texture features of surface image data. IEEE Conference on Prognostics and Health Management (PHM) IEEE, (2014) 1-5

[12] A. A. Kassim, M. A. Mannan, Z. Mian, Texture analysis methods for tool condition monitoring. Image and Vision Computing, 25.7 (2007) 1080-1090.

[13] A. A. Kassim, Z. Mian, M. A. Mannan, Connectivity oriented fast Hough transform for tool wear monitoring. Pattern Recognition, 37.9 (2004) 1925-1933.

[14] D. C. He, L. Wang, Texture unit, texture spectrum, and texture analysis. IEEE transactions on Geoscience and Remote Sensing, 28.4 (1990) 509-512.

[15] D. M. Tsai, J. J. Chen, J. F. Chen, A vision system for surface roughness assessment using neural networks. The International Journal of Advanced Manufacturing Technology, 14.6 (1998) 412-422.

[16] ISO 8688-2:1989. Tool life testing in milling—part 2: end milling.

[17] U. Garcia, M. V. Ribeiro, Ti6Al4V titanium alloy end milling with minimum quantity of fluid technique use. Materials and Manufacturing Processes, 31(7), (2016) 905-918.

[18] W. Polini, S. Turchetta, Cutting force, tool life and surface integrity in milling of titanium alloy Ti-6Al-4V with coated carbide tools. Proceedings of the Institution of Mechanical Engineers, Part B: Journal of Engineering Manufacture, 230(4), (2016) 694-700.

[19] N. Arunachalam, B. Ramamoorthy, Texture analysis for grinding wheel wear assessment using machine vision. Proceedings of the Institution of Mechanical Engineers, Part B: Journal of Engineering Manufacture, 221.3 (2007) 419-430.

[20] M. A. Younis, On line surface roughness measurements using image processing towards an adaptive control. Computers & industrial engineering, 35.1-2 (1998) 49-52.

[21] R. E. Kalman, A new approach to linear filtering and prediction problems. Journal of basic Engineering, 82.1 (1960) 35-45.

[22] G. Bishop, G. Welch, An introduction to the kalman filter. Proc of SIGGRAPH, Course 8, no. 27599-23175 (2001) 41.

[23] H. C. Möhring, K. M. Litwinski, O. Gümmer, Process monitoring with sensory machine tool components. CIRP Annals-Manufacturing Technology, 59.1 (2010) 383-386.

[24] F. A. Niaki, D. Ulutan, L. Mears. In-Process Tool Flank Wear Estimation in Machining Gamma-Prime Strengthened Alloys Using Kalman Filter. Procedia Manufacturing, 1 (2015) 696-707.